Brief Communication

MOLECULAR METABOLISM

RGS2: A multifunctional signaling hub that balances brown adipose tissue function and differentiation

Katarina Klepac [1,2,], JuHee Yang [1,2], Staffan Hildebrand [1], Alexander Pfeifer [1,2,3,*]**

ABSTRACT

Objective: Recruitment of brown adipose tissue (BAT) is a potential new strategy for increasing energy expenditure (EE) to treat obesity. G protein—coupled receptors (GPCRs) represent promising targets to activate BAT, as they are the major regulators of BAT biological function. To identify new regulators of GPCR signaling in BAT, we studied the role of Regulator of G protein Signaling 2 (RGS2) in brown adipocytes and BAT.
Methods: We combined pharmacological and genetic tools to investigate the role of RGS2 in BAT *in vitro* and *in vivo*. Adipocyte progenitors were isolated from wild-type (WT) and RGS2 knockout (RGS2−/−) BAT and differentiated to brown adipocytes. This approach was complemented with knockdown of RGS2 using lentiviral shRNAs (shRGS2). Adipogenesis was analyzed by Oil Red O staining and by determining the expression of adipogenic and thermogenic markers. Pharmacological modulators and fluorescence staining of F-acting stress fibers were employed to identify the underlying signaling pathways. *In vivo*, the activity of BAT was assessed by *ex vivo* lipolysis and by measuring whole-body EE by indirect calorimetry in metabolic cages.
Results: RGS2 is highly expressed in BAT, and treatment with cGMP—an important enhancer of brown adipocyte differentiation—further increased RGS2 expression. Loss of RGS2 strongly suppressed adipogenesis and the expression of thermogenic genes in brown adipocytes. Mechanistically, we found increased Gq/Rho/Rho kinase (ROCK) signaling in the absence of RGS2. Surprisingly, *in vivo* analysis revealed elevated BAT activity in RGS2-deficient mice that was caused by enhanced Gs/cAMP signaling.
Conclusion: Overall, RGS2 regulates two major signaling pathways in BAT: Gq and Gs. On the one hand, RGS2 promotes brown adipogenesis by counteracting the inhibitory action of Gq/Rho/ROCK signaling. On the other hand, RGS2 decreases the activity of BAT through the inhibition of Gs signaling and cAMP production. Thus, RGS2 might represent a stress modulator that protects BAT from overstimulation.

Keywords Regulator of G protein signaling 2; G protein—coupled receptors; Gq; Gs; Brown adipose tissue

1. INTRODUCTION

Almost a decade ago, several laboratories located across different continents reported that adult humans possess active brown adipose tissue (BAT) and that BAT activity is inversely correlated with body mass index in human adults [1—4], a finding that ignited intense research on its therapeutic potential [5,6]. BAT generates heat through the uniquely expressed uncoupling protein-1 (UCP1), which disrupts the proton gradient of the respiratory chain, thereby inhibiting adenosine triphosphate synthesis and generating heat [7,8]. Numerous studies conducted in humans and rodents have shown that BAT contributes to whole-body energy expenditure (EE) and improves metabolic health [5,6,9—11]. Thus, the recruitment and activation of BAT is a promising approach for the treatment of obesity, diabetes, and other metabolic diseases [6,10,12].

The most important regulators of BAT activity include members of the G protein—coupled receptors (GPCRs), a large family of seven-transmembrane receptors [13]. GPCRs regulate vital physiological functions in virtually every tissue, and approximately one-third of the currently approved drugs target GPCR [14,15], making them the largest family of "druggable" proteins [16]. However, not much is known about GPCR signaling in BAT. GPCRs can be divided into four major groups depending on the α subunit of the G protein they couple to: Gs-, Gi-, Gq-, or G12/13-coupled GPCRs [17,18]. The most extensively studied GPCRs in BAT belong to the group of Gs-coupled receptors because they stimulate BAT activity and EE [19,20]. Mechanistically, the activation of Gs-GPCRs, such as β-adrenergic receptors [7] or adenosine A_{2A} receptor [21], results in the stimulation of adenylyl cyclases (ACs) that produce cyclic adenosine-3′,5′-monophosphate (cAMP) [19]. The main target of cAMP is protein kinase A (PKA), which,

[1]Institute of Pharmacology and Toxicology, University of Bonn, 53127 Bonn, Germany [2]Research Training Group 1873, University of Bonn, 53127 Bonn, Germany [3]PharmaCenter, University of Bonn, 53127 Bonn, Germany

*Corresponding author. Institute of Pharmacology and Toxicology, University of Bonn, 53127, Bonn, Germany. E-mail: alexander.pfeifer@uni-bonn.de (A. Pfeifer).

**Corresponding author. Institute for Diabetes and Cancer, Helmholtz Center Munich, 85764, Neuherberg, Germany. E-mail: katarina.klepac@helmholtz-muenchen.de (K. Klepac).

Received August 1, 2019 • Revision received September 12, 2019 • Accepted September 28, 2019 • Available online 5 October 2019

https://doi.org/10.1016/j.molmet.2019.09.015

among other targets, phosphorylates hormone-sensitive lipase (HSL) to induce lipolysis and UCP1-mediated thermogenesis [7,22].
In addition, BAT expresses a broad spectrum of other GPCRs, including several Gq-coupled receptors [23,24]. The role of Gq signaling in BAT is still not clear, and conflicting data have been published: a recent paper claimed that GPR120, a receptor that can couple to Gq [25], promotes metabolic health [24], which is in stark contrast to the finding that the stimulation of Gq inhibits brown adipocyte differentiation and BAT function [23] as well as browning of white adipocytes [26]. To address this point and to decipher intracellular Gq signaling pathways in BAT, we focused on Regulators of G Protein Signaling (RGS), which are important modulators of GPCR activity [27]. RGS function as GTPase-activating proteins (GAPs); they promote GTP hydrolysis by the Gα subunit of G protein, thereby rapidly switching off GPCR signaling [27,28]. They are ubiquitously expressed, and each cell type normally expresses several different RGS proteins [28].
RGS2 is one of the most extensively studied proteins of the RGS family. RGS2 preferentially inhibits the signaling of Gq-coupled GPCRs and is involved in many important physiological processes such as regulation of blood pressure, cardiac remodeling, and immune responses [29–31]. Although RGS2 has strong selectivity for Gq signaling, it was also shown to regulate Gi and Gs signaling, the latter through a GAP-independent mechanism by directly inhibiting ACs [32–34]. The attenuation of Gs signaling by RGS2 plays a role in platelet formation and signal transduction in olfactory neurons [34,35]; however, the physiological significance of Gs inhibition by RGS2 in metabolism is still largely unknown. Human studies have shown that deregulation of RGS2 is associated with hypertension and susceptibility to metabolic syndrome [36,37].
The aim of this study was to elucidate the role of RGS2 in brown adipocyte differentiation and BAT function. RGS2-deficient (RGS2−/−) brown adipocytes exhibited a severe defect in adipogenesis that was caused by increased Gq signaling. Analysis of RGS2−/− mice revealed an unexpected increase in lipolysis and BAT activity due to increased Gs signaling. Thus, RGS2 is a multifunctional inhibitor of Gq that also regulates Gs signaling in BAT.

2. RESULTS

2.1. Expression of RGS2 in fat tissues and isolated brown adipocytes

To study the function of RGS2 in relation to Gq signaling in BAT, we first analyzed the expression of RGS2 in all larger fat depots: BAT, inguinal white adipose tissue (WATi), and gonadal white adipose tissue (WATg). Although RGS2 was present in all fat depots, its expression was by far highest in BAT: 13.6-fold and 7.4-fold higher than the expression in WATi and WATg (Suppl. Fig. 1A). We then measured the mRNA levels of RGS2 in a mouse model of diet-induced obesity. The expression of RGS2 in mice fed a high-fat diet (HFD) was significantly altered ($P < 0.05$) only in BAT, where we found a 59% lower expression than that in the controls fed a chow diet (Suppl. Fig. 1A). We next analyzed RGS2 levels in brown adipocytes differentiated *in vitro*. We found that RGS2 was expressed in both preadipocytes and mature brown adipocytes and that the levels of RGS2 were drastically increased (21.2-fold) during brown adipocyte differentiation, implicating a role in brown adipogenesis (Suppl. Fig. 1B).

2.2. Knockout and knockdown of RGS2 inhibit brown adipogenesis

To analyze whether RGS2 is essential for brown adipocyte differentiation, we isolated preadipocytes from wild-type (WT) and RGS2−/− littermate mice and differentiated them to mature brown adipocytes *in vitro*. Knockout of RGS2 (Suppl. Fig. 1C) completely abolished brown adipocyte differentiation, shown in the reduced Oil Red O staining of lipid droplets (Figure 1A and Suppl. Fig 1D). Western blot analysis revealed decreased expression of the adipogenic markers aP2 and PPARγ in the RGS2−/− cells (by 79% and 59%, respectively) (Figure 1B–C), and the expression of the thermogenic marker UCP1 was reduced by 70% (Figure 1B–C). As a second genetic approach to achieve loss of function, we used a lentiviral small hairpin RNA (shRNA) directed against RGS2. Similar to the RGS2−/− model, knockdown of RGS2 by ∼63% (Suppl. Fig. 1E) resulted in reduced differentiation, with fewer lipid droplets (Figure 1A and Suppl. Fig. 1F) as well as reduced expression of adipogenic and thermogenic markers in the shRGS2 cells than the control cells (aP2, 80%; PPARγ, 85%; UCP1, 65%) (Figure 1D–E). These data indicate that RGS2 plays a vital role in promoting brown adipocyte differentiation.

2.3. Differentiation of RGS2−/− cells can be rescued by Gq knockdown

The main role of RGS2 is to inhibit the signaling of GPCRs coupled to the Gq protein [31]. To investigate whether the impaired phenotype of RGS2−/− cells originates from the overactive Gq signaling, we knocked down Gq using lentiviral shRNA directed against Gq (shGq). Knockdown of Gq in RGS2−/− cells by ∼50% (Suppl. Fig. 1G) restored the differentiation of brown adipocytes, observed in the increased lipid accumulation (Figure 2A and Suppl. Fig. 1H). In addition, shGq enhanced the expression of adipogenic (aP2, 4.1-fold; PPARγ, 9.7-fold) and thermogenic (UCP1, 2.5-fold) markers as compared to the control RGS2−/− cells (Figure 2B–C). Moreover, shGq increased the differentiation of WT cells (Figure 2A–C), further underlining the negative effect of endogenous/paracrine [23] Gq signaling on brown adipogenesis.

2.4. Enhanced Rho/Rho kinase (ROCK) signaling in the absence of RGS2

The RhoA/ROCK pathway is a known downstream target of Gq signaling [38,39]. Moreover, we and others have reported that RhoA/ROCK has negative effects on brown adipocyte differentiation [23,40,41]. As RhoA is associated with the organization and formation of cell cytoskeleton [42], we analyzed F-actin stress fibers in WT and RGS2−/− cells. Phalloidin staining of actin filaments showed increased formation of stress fibers in RGS2−/− cells, pointing to increased Rho activity in these cells (Figure 3A). In addition, treatment with the selective ROCK inhibitor Y-27632 (10 μM) completely restored the differentiation of RGS2−/− cells, which was reflected in increased Oil Red O staining (Figure 3B and Suppl. Fig. 1I) and increased expression of adipogenic and thermogenic markers when compared with that of nontreated RGS2−/− cells (aP2, 15.1-fold; PPARγ, 24.7-fold; UCP1, 14.7-fold) (Figure 3C–D). These results indicate that enhanced Rho/ROCK signaling is responsible for the impaired differentiation of RGS2−/− cells.

2.5. RGS2/cGMP crosstalk in brown adipocytes

Cyclic guanosine-3′,5′-monophosphate (cGMP) is a cyclic nucleotide that plays a key role in the regulation of adipogenic differentiation [6,43]. cGMP has been shown to inhibit RhoA/ROCK signaling in brown adipocytes, thus promoting brown adipogenesis [40]. In addition, direct activation of RGS2 by the cGMP signaling pathway has been reported for vascular smooth muscle cells [30]. We therefore studied the effects of cGMP on the differentiation of RGS2−/− brown adipocytes. Treatment with cGMP (8-Br-cGMP, 200 μM) increased RGS2 expression in WT cells by 2.0-fold (Figure 4A), indicating an additional

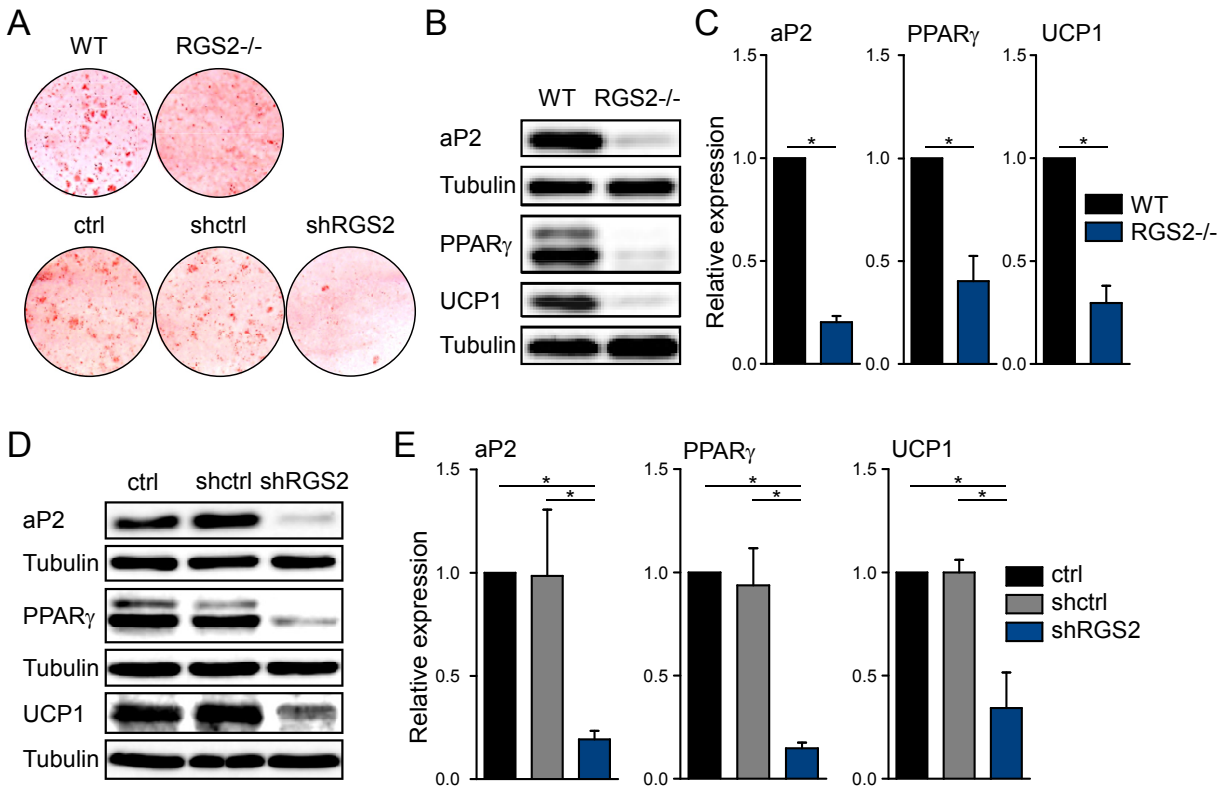

Figure 1: RGS2 is indispensable for brown adipocyte differentiation. (A) Oil Red O stain of WT and RGS2−/− brown adipocytes (upper panel) and Oil Red O stain of brown adipocytes after shRNA-mediated RGS2 knockdown (lower panel). n = 3. (B, C) Representative immunoblots (B) and quantification (C) of adipogenic markers aP2, PPARγ, and thermogenic marker UCP1 in WT and RGS2−/− cells. n = 6. (D, E) Representative immunoblots (D) and quantification (E) of aP2, PPARγ, and UCP1 in brown adipocytes after shRNA-mediated RGS2 knockdown. n = 3. Expression data were normalized to tubulin and are represented as mean ± SEM. (C) *t*-test, $*P < 0.05$. (E) ANOVA, $*P < 0.05$.

mechanism of interaction between RGS2 and cGMP signaling in brown adipocytes. We then analyzed the effects of cGMP on the differentiation of brown adipocytes. In line with the previously published data [40], cGMP increased the differentiation of WT cells (Figure 4B–D and Suppl. Fig. 1J). This was seen in increased lipid droplet accumulation (Figure 4B and Suppl. Fig. 1J) and the expression of aP2, PPARγ, and UCP1 (by 2.3-fold, 4.4-fold, and 7.5-fold, respectively) (Figure 4C–D). Importantly, cGMP rescued the differentiation of RGS2−/− brown adipocytes, as shown by increased Oil Red O staining as well as by enhanced protein expression of the adipogenic markers aP2 (9.4-fold) and PPARγ (20.1-fold), and the thermogenic marker UCP1 (23.2-fold) as compared to the untreated RGS2−/− cells (Figure 4B–D and Suppl. Fig. 1J). These results point to a crosstalk between RGS2 and cGMP in brown adipocytes, both of which synergistically inhibit Gq/RhoA/ROCK signaling at different levels to promote brown adipogenesis.

2.6. Increased Gs signaling and BAT activation in RGS2−/− mice

To study the role of RGS2 in BAT *in vivo*, we analyzed RGS2−/− mice. We found significantly lower body weight in 14- to 18–month-old RGS2−/− mice (Figure 5A), which is in line with previously published data [44] showing that RGS2−/− mice are resistant to age-related weight gain. The weight of BAT, WATi, and WATg depots in RGS2−/− mice was reduced by 13%, 34%, and 52%, respectively, as compared to WT mice, albeit significantly ($P < 0.05$) for only WATg (Figure 5A). However, our *in vitro* data clearly show that loss of RGS2 inhibits brown adipocyte differentiation because of increased Gq signaling. Thus, one would expect reduced BAT activity and increased weight gain in RGS2−/− mice. To address this discrepancy, we focused on the Gs signaling pathway. RGS2 has been shown to inhibit Gs in several different cell types such as murine embryonic fibroblasts, olfactory neurons, and platelets [32,34,35]. In brown adipocytes, the Gs pathway is a major regulator of lipolysis and thermogenesis [12]. We therefore measured lipolysis in the BAT of WT and RGS2−/− mice to study whether loss of RGS2 results in enhanced Gs signaling and activation of BAT. Importantly, BAT activity was increased by 2.3-fold in RGS2−/− mice when compared with that in WT animals (Figure 5B). Moreover, we analyzed the expression of ACs, in particular isoforms III and VI, which are the dominant isoforms in BAT [45,46]. AC III and AC VI expression was significantly ($P < 0.05$) increased (by 2.1-fold and 2.0-fold, respectively) in RGS2−/− BAT (Figure 5C). In addition, we found increased levels of phosphorylated (i.e., active) HSL in the BAT of RGS2−/− mice when compared with their WT controls (Figure 5D). *In vitro*, we found that RGS2−/− cells produced more cAMP after treatment with the direct AC stimulator forskolin (Suppl. Fig. 1K). Overall, these data indicate that loss of RGS2 in BAT leads to increased Gs signaling, which promotes lipolysis and BAT activation.

The primary physiological stimulus for BAT activation is cold stress, which acts through the sympathetic nervous system and norepinephrine release to activate adrenergic receptors and the downstream Gs pathway [19]. Therefore, we exposed mice to cold stress and studied BAT activation by indirect calorimetry. Cold-exposed RGS2−/− mice had significantly ($P < 0.05$) increased whole-body EE when compared with the WT controls (Figure 5E). This was accompanied by

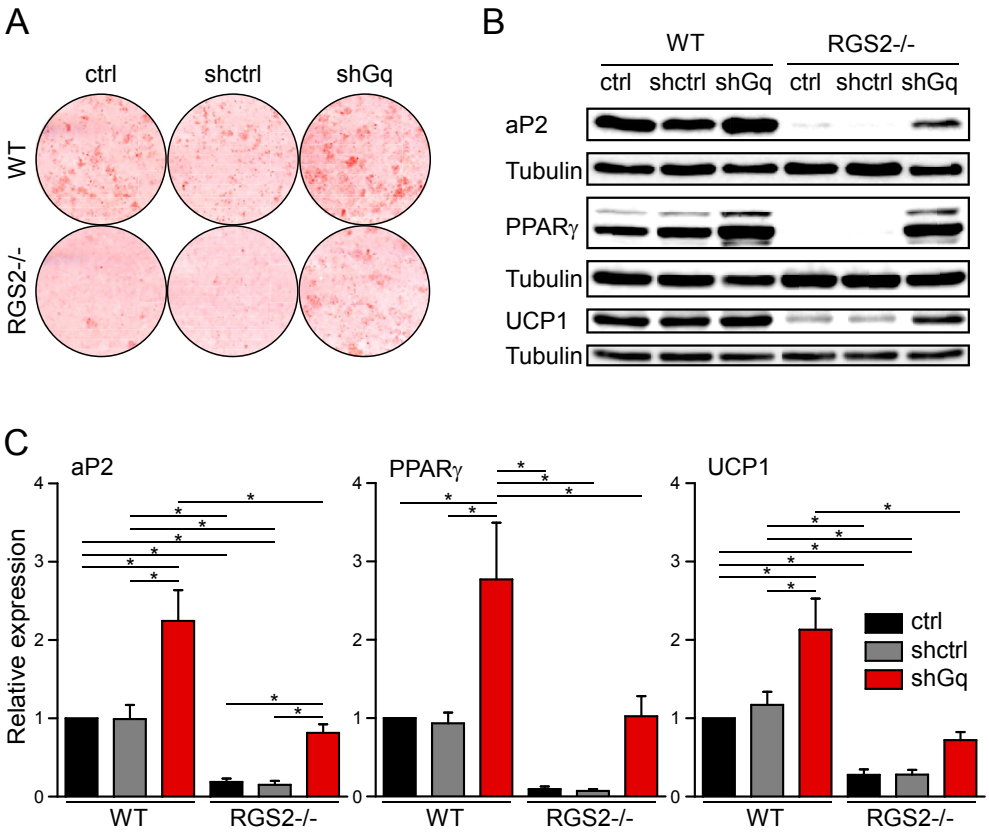

Figure 2: Enhanced Gq signaling is responsible for the impaired differentiation of RGS2−/− cells. (A) Oil Red O stain of nontransduced cells (ctrl) and cells transduced with control virus (shctrl) or shRNA-directed against Gq (shGq) in WT and RGS2−/− cells. n = 3. (B, C) Representative immunoblots (B) and quantification (C) of adipogenic markers aP2, PPARγ, and thermogenic marker UCP1 in ctrl, shctrl, or shGq in WT and RGS2−/− cells. n = 5. Expression data were normalized to tubulin and are represented as mean ± SEM. ANOVA, $*P < 0.05$.

a significant ($P < 0.05$) decrease in the body weight of RGS2−/− mice by 9% (Figure 5E).

Taken together, our data show that RGS2 is a major regulator of BAT differentiation and function. RGS2 seems to release the break of BAT differentiation caused by Gq signaling and also has an inhibitory effect on Gs, possibly to avoid the overstimulation of BAT and excessive dissipation of energy in the form of heat (Figure 6).

3. DISCUSSION

RGS proteins are important regulators of GPCR signaling in a broad spectrum of cells [27]. RGS proteins enhance the GTPase activity of the Gα subunit, thereby returning the activated G protein to its inactive state and rapidly shutting down GPCR signaling [27]. RGS2 primarily targets the activity of the Gαq protein [31]; however, RGS2 can also interact with other components of GPCR signaling, including ACs as well as a broad range of other cellular signaling components, including ion channels and kinases [47].

In this study, we focused on the role of RGS2 in BAT because of its importance for Gq signaling and its diverse effects on GPCR signaling pathways. GPCR signaling governs major processes in brown adipocytes: differentiation and function [19,21,23].

Analysis of RGS2 expression showed high abundance in all larger fat depots, with the highest levels detected in BAT. Downregulation or a complete knockout of RGS2 in preadipocytes isolated from BAT abolished adipogenic and thermogenic differentiation, revealing an important role of RGS2 in the control of brown adipogenesis. A previous study [44] that analyzed RGS2−/− white adipocytes *in vitro* found decreased expression of adipogenic markers, indicating that RGS2 is essential for both brown adipocyte and white adipocyte differentiation.

To identify the underlying mechanism, we focused on Gq signaling as the primary target of RGS2 [31]. Our group has recently shown that Gq signaling has a negative impact on brown adipocyte differentiation [23]. However, the exact role of Gq in brown cells and brown-like cells in WAT (beige adipocytes) [48] is still under discussion. Recent reports have shown that the inhibition of the Gq-coupled GPCR endothelin receptor type A and serotonin receptor type 2A in brown and beige adipocytes improves metabolic health [23,26]. In contrast, acute stimulation of free fatty acid receptor 4 (FFA4/GPR120), which can also signal through Gq [25], using TUG-891 had beneficial effects on metabolism by stimulating mitochondrial respiration in brown adipocytes [24]. Although TUG-891 is a potent and selective agonist of the human FFA4/GPR120 receptor, its selectivity is reduced for the mouse GPR120 receptor [49]. Thus, the differences observed might be due to selectivity issues with this agonist [49]. Here, we found that the knockdown of Gq restored the adipogenic and thermogenic potential of RGS2−/− brown adipocytes, suggesting that RGS2 controls brown adipocyte differentiation through the inhibition of the Gq protein.

RGS2 can regulate Gq through multiple mechanisms [28,50]: RGS2 can hydrolyze G protein—bound GTP, thereby inactivating Gq signaling [28]. In addition, RGS2 promotes the dissociation of Gαq and its

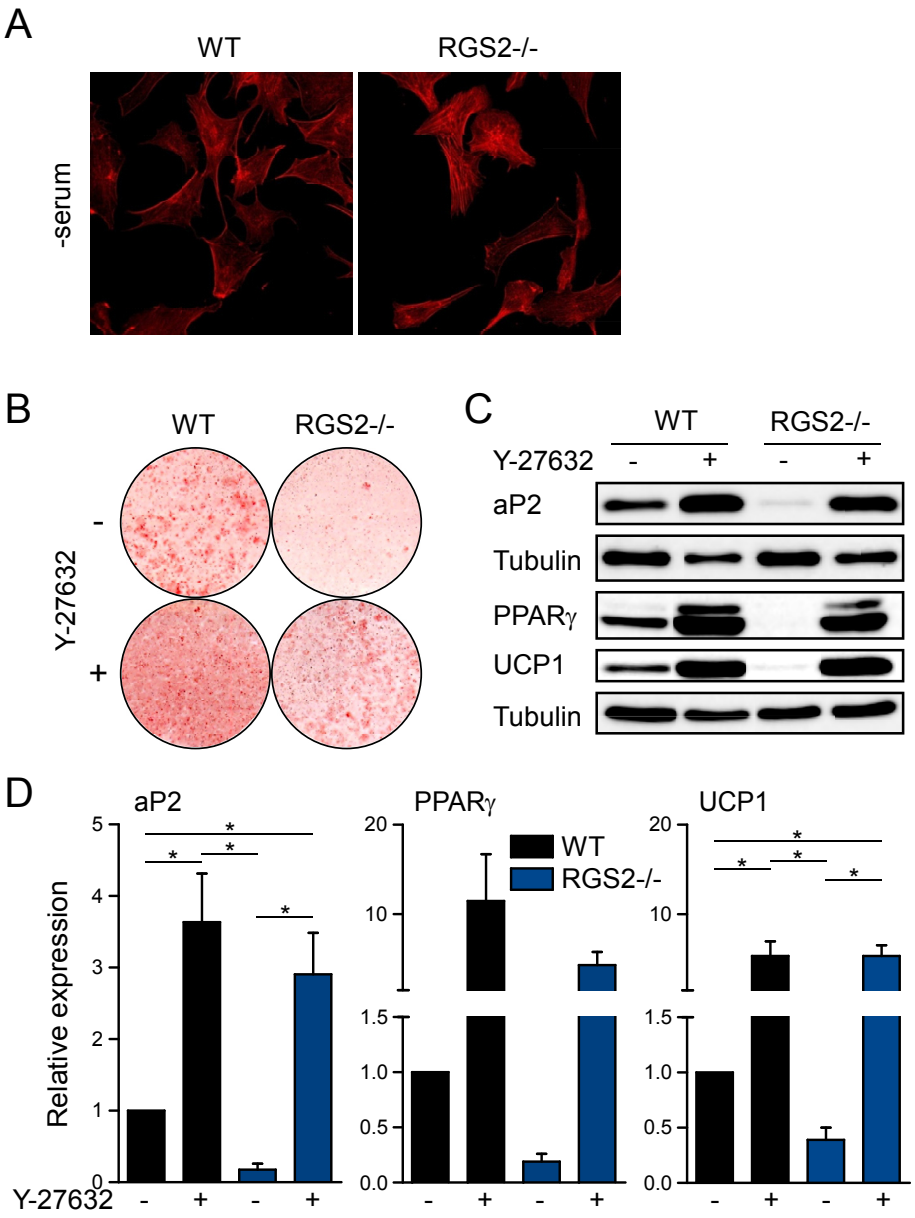

Figure 3: Inhibition of Rho/ROCK restores the phenotype of RGS2−/− cells. (A) Phalloidin staining of F-actin stress fibers in WT and RGS2−/− cells. n = 3. (B) Oil Red O-stained WT and RGS2−/− cells differentiated in the presence or absence of the ROCK inhibitor Y-27632 (10 μM). n = 3. (C, D) Representative immunoblots (C) and quantification (D) of the adipogenic markers aP2 and PPARγ and the thermogenic marker UCP1 in WT and RGS2−/− cells differentiated in the presence or absence of Y-27632. n = 3. Expression data were normalized to tubulin and are represented as mean ± SEM. ANOVA, $*P < 0.05$.

downstream effector p63RhoGEF, which is a Gq-specific Rho GTPase involved in the regulation of RhoA activity [50]. RhoA is a small G protein that belongs to the superfamily of Ras and is involved in cytoskeleton regulation [51] primarily by interacting with ROCKs [52], serine-threonine kinases that suppress brown adipogenesis [40].

To understand the mechanism of impaired differentiation in RGS2−/− brown adipocytes, we focused on Rho/ROCK signaling. Analysis of RGS2−/− cells showed increased formation of stress fibers, indicating increased activity of Rho in these cells. Importantly, inhibition of ROCK rescued the differentiation of RGS2−/− cells, suggesting that enhanced Rho/ROCK signaling is responsible for the differentiation defect. Although other members of the Rho family can also affect stress fiber formation [53], the differentiation of RGS2−/− is presumably regulated through RhoA, which is a well-established negative regulator of adipogenic differentiation [40,54].

One of the major regulators of RhoA activity in brown adipocytes is the cGMP signaling pathway [40]. cGMP induces the phosphorylation of RhoA through its downstream target protein kinase G (PKG) [40]. Treatment of RGS2−/− cells with cGMP completely restored brown adipocyte differentiation, possibly through the inhibition of RhoA, although cGMP can promote brown adipogenesis through multiple mechanisms [55]. Moreover, cGMP treatment induced RGS2 expression in WT cells. This could represent an additional mechanism through which cGMP inhibits Gq signaling and thereby promotes brown adipogenesis. A crosstalk between RGS2 and the cGMP pathway has previously been reported in other cell types [30]. In vascular smooth

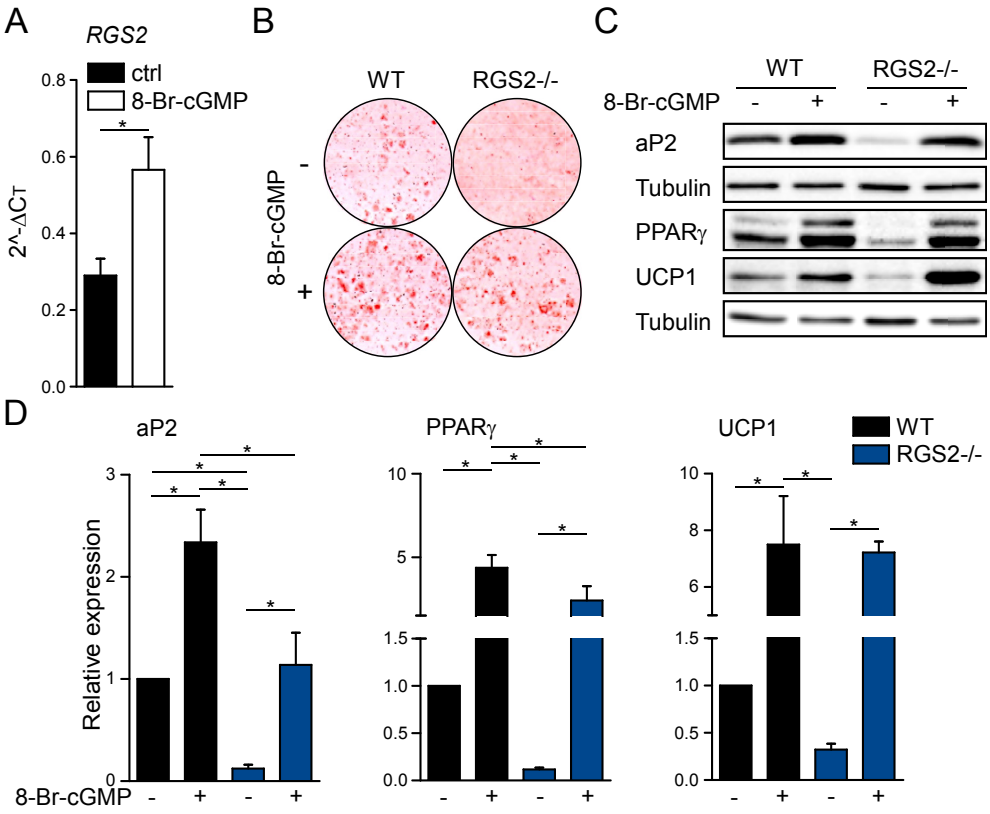

Figure 4: cGMP/RGS2 crosstalk in brown adipocytes. (A) mRNA expression of RGS2 in WT cells differentiated in the presence or absence of 8-Br-cGMP (200 μM). n = 9. (B) Oil Red O-stained WT and RGS2−/− cells differentiated in the presence or absence of 8-Br-cGMP (200 μM). n = 3. (C, D) Representative immunoblots (C) and quantification (D) of the adipogenic markers aP2, PPARγ, and thermogenic marker UCP1 in WT and RGS2−/− cells differentiated in the presence or absence of 8-Br-cGMP. n = 3. Expression data were normalized to tubulin for protein levels and to HPRT for mRNA levels and are represented as mean ± SEM. (A) *t*-test, $*P < 0.05$. (D) ANOVA, $*P < 0.05$.

muscle cells, it has been shown that nitric oxide induces the production of cGMP, which activates PKG [30,56]. Importantly, PKG can directly phosphorylate and activate RGS2, which attenuates the contraction of vascular smooth muscle cells through the inhibition of Gq [30,56]. Thus, the crosstalk between the Gq/RGS2 and the cGMP pathway might regulate brown adipogenesis at different levels.

We further analyzed the role of RGS2 in BAT *in vivo*. Given the dramatic effect of RGS2 deficiency on brown adipocyte differentiation, one would expect reduced BAT-dependent EE and weight gain. In contrast, RGS2−/− mice had in fact improved metabolic parameters, reflected in reduced blood triglycerides and faster glucose clearance [44]. Moreover, Nunn et al. [44] and our group found that RGS2−/− mice are resistant to weight gain during aging. Our data showed a reduction in the body weight of 14- to 18-month-old RGS2−/− mice, accompanied by a significant decrease in the weight of WATg by 52%. These differences between the *in vitro* and the *in vivo* phenotype prompted us to study additional pathways potentially targeted by RGS2 in brown adipocytes.

Previous studies have shown that RGS2 can also inhibit Gs signaling, a major driver of BAT lipolysis and thermogenesis [10], in several cell types including white adipocytes and osteoblasts [32,57]. RGS2 can regulate cAMP signaling independently from the GAP mechanism through direct interaction with AC, in particular with isoforms III, V, and VI [32,34,58]. Notably, AC isoforms III and VI are abundantly expressed in BAT (Figure 5C) [45,46]. Consistent with the proposed role of RGS2 as an AC inhibitor, lipolysis was significantly increased in RGS2−/− BAT. Moreover, the level of phosphorylated HSL—the major downstream target of cAMP/PKA in adipocytes—was also elevated. Our data also show that RGS2 affects the expression of AC isoforms III and VI, presenting an additional mechanism of the RGS2 inhibition of Gs signaling in BAT. *In vitro*, we found increased cAMP levels in RGS2−/− cells stimulated with forskolin. These alterations in Gs/AC signaling can also explain the increase in whole-body EE in RGS2−/− mice, which could originate from the lack of this inhibitory effect of RGS2 on Gs. RGS2 could thus alleviate the overstimulation of BAT thermogenesis under long-term cold stimulation or chronic pharmacological activation.

As Gs/cAMP signaling has been shown to increase brown adipocyte differentiation [7], higher activity of Gs/cAMP found in the BAT of RGS2−/− mice *in vivo* could counteract the detrimental effects of Gq on brown adipocyte differentiation. In contrast, we did not observe increased basal cAMP levels in RGS2−/− preadipocytes, indicating that *in vitro*, the basal stimulation of Gs signaling is too low and cannot rescue the Gq-induced impairment of differentiation. In addition, because of the expression of RGS2 in a variety of tissues, including the brain, lung, and heart [59,60], indirect effects on BAT function by other organs in RGS2−/− mice cannot be excluded. Such effects could account for, or contribute to, the observed differences between the *in vitro* and *in vivo* studies.

In conclusion, our results demonstrate that RGS2 is an important regulator of BAT adipogenesis and function through the inhibition of GPCR signaling. *In vitro*, we uncovered a link between RGS2 and the Gq pathway: we found that RGS2−/− brown adipocyte differentiation is impaired due to elevated Gq/Rho/ROCK signaling. Moreover, we

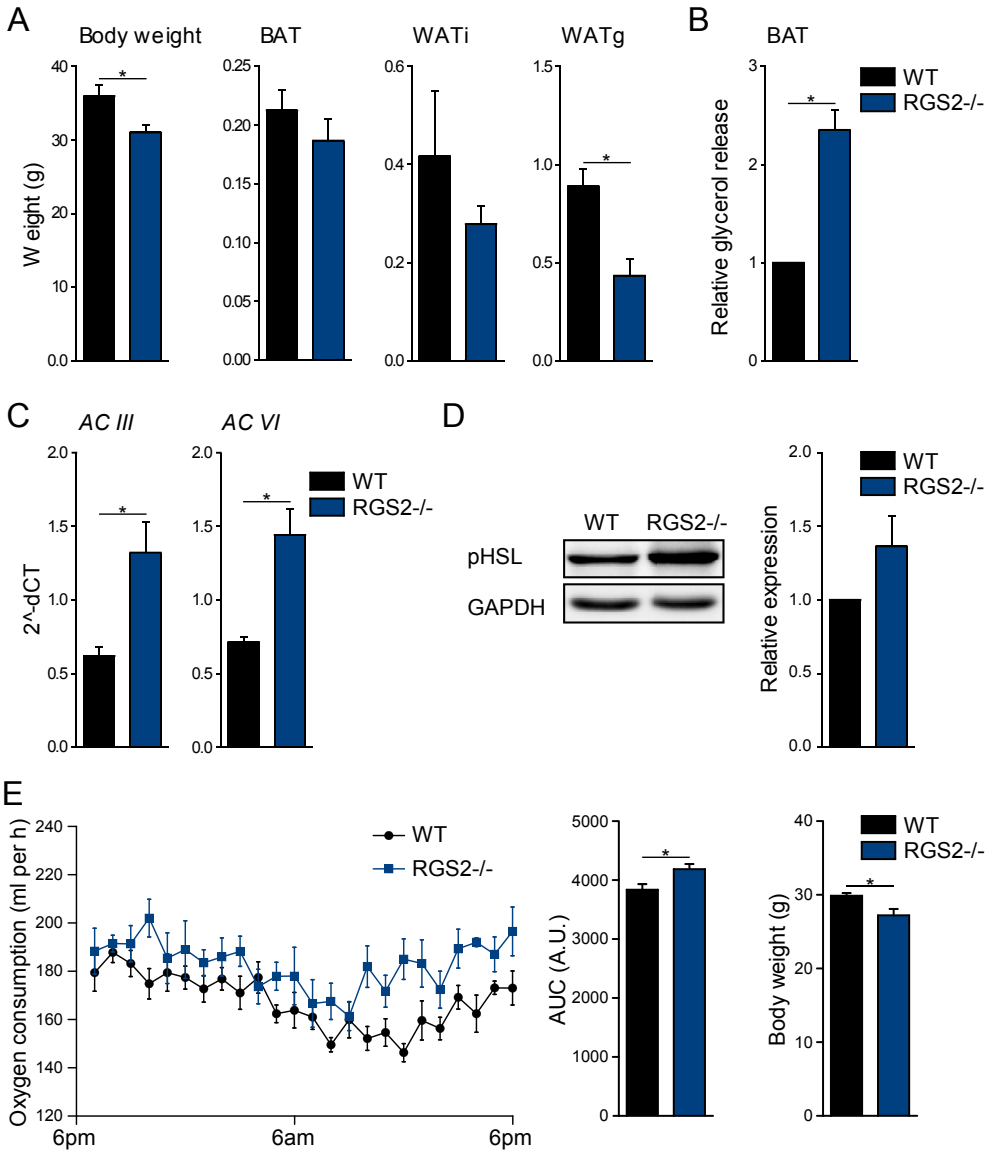

Figure 5: RGS2 inhibits Gs signaling in BAT *in vivo*. (A) Body weights and fat tissue weights of WT and RGS2−/− mice. WT; n = 3, RGS2−/−; n = 5. (B) BAT activation measured as lipolysis (glycerol release) in WT and RGS2−/− mice. WT; n = 3, RGS2−/−; n = 5. (C) mRNA expression of AC III and AC VI in the BAT of WT and RGS2−/− mice. WT; n = 3, RGS2−/−; n = 5. (D) Representative immunoblots and quantification of phosphorylated HSL (pHSL) in the BAT of WT and RGS2−/− mice, normalized to GAPDH. WT; n = 3, RGS2−/−; n = 5. (E) Oxygen consumption over 24 h and area under the curve of WT and RGS2−/− mice at 4 °C. Body weights of cold-exposed WT and RGS2−/− mice. WT; n = 6, RGS2−/−; n = 5. All data are shown as mean ± SEM. *t*-test, $*P < 0.05$.

found a crosstalk between RGS2 and the cGMP pathway, an important promotor of brown adipogenesis. Our data show that RGS2 also inhibits Gs, thereby regulating the activity of BAT and whole-body EE. Overall, the role of RGS2 in metabolism seems complex: RGS2 shifts the balance toward differentiation (inhibition of Gq) and inhibition of BAT overactivation by regulating Gs/AC signaling; therefore, RGS2 might act as a stress modulator in BAT.

4. MATERIALS AND METHODS

4.1. Isolation and immortalization of BAT-derived MSCs

BAT isolated from newborn WT and RGS2−/− littermates was dissected and incubated for 30 min at 37 °C in digestion buffer (Dulbecco's modified Eagle's medium [DMEM], Invitrogen) containing 123 mM Na^+, 5 mM K^+, 1.3 mM Ca^{2+}, 131 mM Cl^-, 5 mM glucose, 1.5% (w/v) bovine serum albumin (BSA), 100 mM HEPES, and 0.2% (w/v) collagenase type II (pH 7.4) in a shaking water bath. The digested tissue was filtered through a 100-μm nylon mesh and incubated for 30 min on ice. The middle phase containing BAT-derived mesenchymal stem cells (MSCs) was collected and filtered through a 30-μm nylon mesh. The filtrate was centrifuged at 700 g for 10 min, and the cell pellet was resuspended in 1 ml of primary cell culture medium (DMEM supplemented with 10% fetal bovine serum [FBS], 100 IU penicillin, streptomycin [100 mg ml^{-1}] [P/S], 4 nM insulin, 4 nM triiodothyronine, 10 mM HEPES, and sodium ascorbate [25 mg ml^{-1}]). The cells were seeded on a 6-well TC plate at a density of ~60,000 cells per cm^2. The next day, the cells were immortalized using lentivirus (200 ng of reverse transcriptase) containing Simian Virus 40

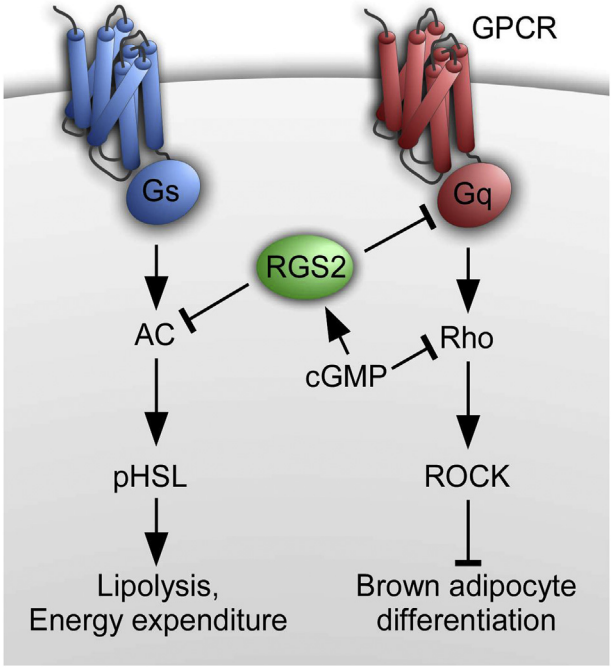

Figure 6: Schematic depiction summarizing the role of RGS2 in brown adipocyte differentiation and function.

(SV40) large T-antigen per well, which was under the control of phosphoglycerate kinase promoter (PGK). Cells were expanded in DMEM supplemented with FBS and P/S (GM).

4.2. Differentiation of brown adipocytes

Approximately 180,000 immortalized cells per well were seeded in GM on a 6-well plate. Forty-eight hours after seeding the cells, GM was replaced with DMEM supplemented with FBS, P/S, 20 nM insulin, and 1 nM triiodothyronine (DM). After another two days, brown adipogenesis was stimulated with induction medium (DM supplemented with 0.5 mM isobutylmethylxanthine [IBMX] and 1 mM dexamethasone). Two days after the induction, the cells were cultured in DM for another 5 days. Where indicated, starting 48 h after seeding, the cells were treated every second day with 200 μM 8-Br-cGMP (BioLog) or 10 μM Y-27632 (Tocris). For experiments with preadipocytes, the cells were analyzed 48 h after seeding (preadipocytes). For experiments with mature brown adipocytes, the cells were analyzed 7 days after induction (brown adipocytes).

4.3. Lentiviral infection

HEK293T cells were transfected with vector constructs and packaging plasmids to produce lentiviral particles, which were concentrated by ultracentrifugation [40,61]. Lentiviral infection of brown adipocytes was achieved as follows: cells were seeded on 6-well TC plates at a density of ~180,000 cells/well. Eight hours after seeding, 100 ng of shRGS2 (Sigma), shGq (Sigma), or shctrl lentivirus, quantified by reverse transcriptase—enzyme-linked immunosorbent assay (ELISA), was added to preadipocytes, and the cells were incubated overnight at 37 °C, 5% CO_2. The cells were differentiated to mature brown adipocytes as described above. shRNA lentiviral constructs were expressed under the control of the U6 promoter (pLKO.1-U6-sh-ctrl sequence: 5′-GCATGCAGAAGTGTAAAGCTA-3′, pLKO.1-U6-sh-RGS2-54761-PGK-Puro sequence: 5′- CCTCGGTTCTTGGAGTCCGAA-3′, pLKO.1-U6-sh-Gq-287918-PGK-Puro sequence: 5′-GCTTGTGGAATGATCCTGGAA-3′).

4.4. cAMP measurements

WT and RGS2−/− brown preadipocytes were seeded in GM on a 6-well plate. After 48 h, cells were treated with DMSO or 1 μM forskolin (Sigma) for 15 min. Cells were lysed using 0.1 M HCl, and cAMP levels were determined using a direct cAMP ELISA kit (Enzo Life Sciences) according to the manufacturer's instructions. Protein levels were determined using a Pierce BCA protein assay kit (Thermo Fisher Scientific), and the results were normalized to protein content.

4.5. Protein extraction and western blot analysis

To prepare lysates from cell cultures and tissues, we used lysis buffer (50 mM Tris [pH 7.5], 150 mM NaCl, 1% NP-40, 0.5% sodium deoxycholate, 0.1% sodium dodecyl sulfate [SDS], 0.1 mM EDTA, and 0.1 mM EGTA) supplemented with complete protease inhibitor cocktail (Roche), 1 mM Na_3VO_4, and 10 mM NaF. Protein concentrations were measured using the Bradford method. Proteins were separated using SDS—polyacrylamide gel electrophoresis and transferred onto a nitrocellulose membrane. After the transfer, the membrane was blocked for 1 h in 5% milk powder in Tris-buffered saline and 0.1% Tween 20 (TBST). After washing in TBST, the membrane was incubated with primary antibody (1:1000) overnight at 4 °C. The next day, the membranes were washed in TBST and incubated with secondary horseradish peroxidase—linked antibodies against goat (Dianova, Cat. No. 705-035-147, 1:5,000), mouse (Dianova, Cat. No. 115-035-146, 1:10,000), or rabbit (Cell Signaling, Cat. No. 7074, 1:5,000) for 1 h at room temperature. The membrane was washed with TBST, and proteins were visualized in an ImageQuant LAS 4000 Mini (GE Healthcare Life Sciences) using Amersham ECL western blotting detection reagent (GE Healthcare Life Sciences). The following primary antibodies were used: aP2 (Santa Cruz Biotechnology, Cat. No. sc-18661), PPARγ (Santa Cruz Biotechnology, Cat. No. sc-7273), UCP1 (Sigma—Aldrich, Cat. No. sc-6529), phospho-HSL (Cell Signaling, Cat. No. 4126), GAPDH (Cell Signaling, Cat. No. 2118), and Tubulin (Dianova, Cat. No. MS-719-P0).

4.6. Housing and genotyping of WT and RGS2−/− mice

Animal studies were approved by Landesamt für Natur, Umwelt und Verbraucherschutz, NRW, Germany. RGS2−/− mice on a C57Bl/6 background were provided by Josef Penninger, Institute of Molecular Biotechnology, Vienna, Austria [30]. Mice were maintained on a daily cycle of 12 h light (0600—1800 h) and 12 h darkness (1800—0600 h), at 24 ± 1 °C, and were allowed free access to standard chow and water. For the HFD experiment, 10-week-old WT male C57Bl/6 mice were purchased from Charles River Laboratory. Mice were fed either HFD (60% energy from fat) or control diet purchased from ssniff for 8 weeks.

To genotype the WT and RGS2−/− litter-matched mice, a small piece of tissue was digested in 500 μL proteinase K buffer (100 mM Tris—HCl; pH 7.6, 200 mM NaCl, 5 mM EDTA, 0.2% SDS, 0.1 mg ml^{-1} Proteinase K; Roche) overnight at 55 °C. The next day, 500 μl phenol/chloroform/isoamyl alcohol (Roti®-Phenol, Carl Roth) was added, and DNA was further isolated according to the manufacturer's instructions. Reverse transcription polymerase chain reaction (RT-PCR) primers used to genotype WT and RGS2−/− mice are listed in Supplementary Table 1. The product sizes obtained using WT and RGS2−/− primers were 586 bp and 693 bp, respectively. For fat tissue analysis, 14- to 18-month-old litter-matched male WT and RGS2−/− mice were used.

4.7. RNA isolation and real-time quantitative RT-PCR (qPCR)

mRNA was isolated using InnuSOLV RNA Reagent (Analytik Jena AG) according to the manufacturer's instructions. A total of 500 ng mRNA was used to synthesize cDNA using Transcriptor First Strand cDNA Synthesis Kit (Roche). qPCR was performed using LightCycler 480 SYBR Green I Master (Roche) and an HT7900 instrument (Applied Biosystems). Hypoxanthine-guanine phosphoribosyltransferase (HPRT) was used as an internal control. Primer sequences are listed in Supplementary Table 2.

4.8. F-actin staining of adherent cells in culture

Glass coverslips were placed in 24-well TC plates and coated with 200 µl fibronectin (Sigma, 5 µg ml^{-1} in phosphate-buffered saline [PBS]). After the coating, wells were washed with PBS, and brown preadipocytes were seeded at a density of ~20,000 cells per well. The next day, the cells were serum-starved for another 24 h. After washing with PBS, the cells were fixed with 4% paraformaldehyde (PFA) in PBS. Preadipocytes were permeabilized using 0.1% Triton-X 100 and blocked with 1% BSA in PBS. After blocking, the cells were stained with Alexa Fluor 546 Phalloidin (Thermo Fisher Scientific; 0.165 µM) at room temperature in the dark. After washing with PBS, coverslips were mounted on glass slides and dried overnight. F-actin fibers were visualized using an Axio Observer.Z1 microscope (Zeiss).

4.9. Oil Red O staining

Brown adipocytes were washed with PBS and fixed in 4% PFA in PBS for 30 min at room temperature. After fixation, the cells were washed with PBS and incubated with the Oil Red O solution (Sigma; 3 mg ml^{-1} in 60% isopropyl alcohol) for 3 h at RT. After staining, the cells were washed with distilled water and visualized under a microscope. Densitometric quantification of Oil Red O staining was performed using ImageJ software. Background correction was performed by applying a fixed binary color threshold to all wells in each experiment.

4.10. Cold exposure and measurement of EE in WT and RGS2−/− mice

Mice were maintained on a daily cycle of 12 h light (0600−1800 h) and 12 h darkness (1800−0600 h), at 24 ± 1 °C, and were allowed free access to standard chow and water. For the cold exposure experiment, 18-month-old male WT and RGS2−/− mice were acclimatized to cold stress for 1 week at 18 °C, followed by 1 week of cold exposure at 4 °C. Oxygen consumption was measured at 4 °C with Phenomaster (TSE).

4.11. Ex vivo lipolysis

BAT isolated from WT and RGS2−/− litter-matched mice was weighed, cut into small pieces, and incubated in 300 µl of lipolysis medium (DMEM Gibco, Cat. No. 21063, supplemented with 2% BSA) for 2 h at 37 °C, 5% CO_2. After incubation, 40 µl of the lipolysis medium was mixed with 60 µl of free glycerol reagent, and the medium was then incubated for 5 min at 37 °C, 5% CO_2. Absorption was measured using the EnSpire multimode plate reader at 540 nm. Total glycerol value was calculated from the value of glycerol standard solution absorption and normalized to the amount of tissue used for the lipolysis.

4.12. Statistical analysis

"n" represents the number of cell cultures grown and differentiated independently or number of mice per group. All data were calculated using GraphPad Prism 5 software and are represented as mean ± standard error of the mean (SEM). Statistical analyses were performed using two-tailed Student's *t*-test for single comparisons or analysis of variance (ANOVA) with Newman−Keuls post-hoc test for multiple comparisons. P values <0.05 were considered significant.

COMPETING FINANCIAL INTEREST

The authors declare no competing financial interest.

AUTHOR CONTRIBUTIONS

K.K. designed and performed experiments, analyzed data, and wrote the manuscript. JH.Y. performed experiments and analyzed data. S.H. analyzed the data. A.P. designed and supervised the experiments and wrote the manuscript.

ACKNOWLEDGMENTS

We thank D. Hass and E. Weidner for expert technical assistance, J. Penninger (Institute of Molecular Biotechnology, Vienna, Austria) for providing RGS2−/− mice. Funded by the Deutsche Forschungsgemeinschaft (DFG, German Research Foundation) − 214362475 / GRK1873/2.

CONFLICT OF INTEREST

None declared.

APPENDIX A. SUPPLEMENTARY DATA

Supplementary data to this article can be found online at https://doi.org/10.1016/j.molmet.2019.09.015.

REFERENCES

[1] van Marken Lichtenbelt, W.D., Vanhommerig, J.W., Smulders, N.M., Drossaerts, J.M., Kemerink, G.J., Bouvy, N.D., et al., 2009. Cold-activated brown adipose tissue in healthy men. New England Journal of Medicine 360(15):1500−1508.

[2] Virtanen, K.A., Lidell, M.E., Orava, J., Heglind, M., Westergren, R., Niemi, T., et al., 2009. Functional brown adipose tissue in healthy adults. New England Journal of Medicine 360(15):1518−1525.

[3] Saito, M., Okamatsu-Ogura, Y., Matsushita, M., Watanabe, K., Yoneshiro, T., Nio-Kobayashi, J., et al., 2009. High incidence of metabolically active brown adipose tissue in healthy adult humans: effects of cold exposure and adiposity. Diabetes 58(7):1526−1531.

[4] Nedergaard, J., Bengtsson, T., Cannon, B., 2007. Unexpected evidence for active brown adipose tissue in adult humans. American Journal of Physiology. Endocrinology and Metabolism 293(2):E444−E452.

[5] Cypess, A.M., Kahn, C.R., 2010. Brown fat as a therapy for obesity and diabetes. Current Opinion in Endocrinology Diabetes and Obesity 17(2):143−149.

[6] Pfeifer, A., Hoffmann, L.S., 2015. Brown, beige, and white: the new color code of fat and its pharmacological implications. Annual Review of Pharmacology and Toxicology 55(1):207−227.

[7] Cannon, B., Nedergaard, J., 2004. Brown adipose tissue: function and physiological significance. Physiological Reviews 84(1):277−359.

[8] Kajimura, S., Saito, M., 2014. A new era in Brown adipose tissue biology: molecular control of Brown fat development and energy homeostasis. Annual Review of Physiology 76(1):225−249.

[9] Lidell, M.E., Betz, M.J., Enerback, S., 2014. Brown adipose tissue and its therapeutic potential. Journal of Internal Medicine 276(4):364−377.

[10] Harms, M., Seale, P., 2013. Brown and beige fat: development, function and therapeutic potential. Nature Medicine 19(10):1252−1263.

[11] Bartelt, A., Heeren, J., 2014. Adipose tissue browning and metabolic health. Nature Reviews Endocrinology 10(1):24—36.
[12] Rosen, E.D., Spiegelman, B.M., 2014. What we talk about when we talk about fat. Cell 156(1—2):20—44.
[13] Lefkowitz, R.J., 2007. Seven transmembrane receptors: something old, something new. Acta Physiologica (Oxf) 190(1):9—19.
[14] Kobilka, B.K., 2011. Structural insights into adrenergic receptor function and pharmacology. Trends in Pharmacological Sciences 32(4):213—218.
[15] Latek, D., Modzelewska, A., Trzaskowski, B., Palczewski, K., Filipek, S., 2012. G protein-coupled receptors–recent advances. Acta Biochimica Polonica 59(4): 515—529.
[16] Sriram, K., Insel, P.A., 2018. GPCRs as targets for approved drugs: how many targets and how many drugs? Molecular Pharmacology.
[17] Pierce, K.L., Premont, R.T., Lefkowitz, R.J., 2002. Seven-transmembrane receptors. Nature Reviews Molecular Cell Biology 3(9):639—650.
[18] Wess, J., 1997. G-protein-coupled receptors: molecular mechanisms involved in receptor activation and selectivity of G-protein recognition. The FASEB Journal 11(5):346—354.
[19] Collins, S., 2011. Beta-adrenoceptor signaling networks in adipocytes for recruiting stored fat and energy expenditure. Frontiers in Endocrinology (Lausanne) 2:102.
[20] Bachman, E.S., Dhillon, H., Zhang, C.Y., Cinti, S., Bianco, A.C., Kobilka, B.K., et al., 2002. betaAR signaling required for diet-induced thermogenesis and obesity resistance. Science 297(5582):843—845.
[21] Gnad, T., Scheibler, S., von Kugelgen, I., Scheele, C., Kilic, A., Glode, A., et al., 2014. Adenosine activates brown adipose tissue and recruits beige adipocytes via A2A receptors. Nature 516(7531):395—399.
[22] Townsend, K.L., Tseng, Y.-H., 2014. Brown fat fuel utilization and thermogenesis. Trends in Endocrinology and Metabolism: TEM 25(4):168—177.
[23] Klepac, K., Kilic, A., Gnad, T., Brown, L.M., Herrmann, B., Wilderman, A., et al., 2016. The Gq signalling pathway inhibits brown and beige adipose tissue. Nature Communications 7:10895.
[24] Schilperoort, M., van Dam, A.D., Hoeke, G., Shabalina, I.G., Okolo, A., Hanyaloglu, A.C., et al., 2018. The GPR120 agonist TUG-891 promotes metabolic health by stimulating mitochondrial respiration in brown fat. EMBO Molecular Medicine.
[25] Hirasawa, A., Tsumaya, K., Awaji, T., Katsuma, S., Adachi, T., Yamada, M., et al., 2005. Free fatty acids regulate gut incretin glucagon-like peptide-1 secretion through GPR120. Nature Medicine 11(1):90—94.
[26] Kristóf, E., Doan-Xuan, Q.M., Sárvári, A.K., Klusóczki, Á., Fischer-Posovszky, P., Wabitsch, M., et al., 2016. Clozapine modifies the differentiation program of human adipocytes inducing browning. Translational Psychiatry 6:e963.
[27] De Vries, L., Zheng, B., Fischer, T., Elenko, E., Farquhar, M.G., 2000. The regulator of G protein signaling family. Annual Review of Pharmacology and Toxicology 40:235—271.
[28] Ross, E.M., Wilkie, T.M., 2000. GTPase-activating proteins for heterotrimeric G proteins: regulators of G protein signaling (RGS) and RGS-like proteins. Annual Review of Biochemistry 69:795—827.
[29] Oliveira-Dos-Santos, A.J., Matsumoto, G., Snow, B.E., Bai, D., Houston, F.P., Whishaw, I.Q., et al., 2000. Regulation of T cell activation, anxiety, and male aggression by RGS2. Proceedings of the National Academy of Sciences of the U S A 97(22):12272—12277.
[30] Tang, K.M., Wang, G.R., Lu, P., Karas, R.H., Aronovitz, M., Heximer, S.P., et al., 2003. Regulator of G-protein signaling-2 mediates vascular smooth muscle relaxation and blood pressure. Nature Medicine 9(12):1506—1512.
[31] Heximer, S.P., Watson, N., Linder, M.E., Blumer, K.J., Hepler, J.R., 1997. RGS2/G0S8 is a selective inhibitor of Gqalpha function. Proceedings of the National Academy of Sciences of the U S A 94(26):14389—14393.
[32] Roy, A.A., Baragli, A., Bernstein, L.S., Hepler, J.R., Hebert, T.E., Chidiac, P., 2006. RGS2 interacts with Gs and adenylyl cyclase in living cells. Cellular Signalling 18(3):336—348.
[33] Chakir, K., Zhu, W., Tsang, S., Woo, A.Y., Yang, D., Wang, X., et al., 2011. RGS2 is a primary terminator of beta(2)-adrenergic receptor-mediated G(i) signaling. Journal of Molecular and Cellular Cardiology 50(6):1000—1007.
[34] Sinnarajah, S., Dessauer, C.W., Srikumar, D., Chen, J., Yuen, J., Yilma, S., et al., 2001. RGS2 regulates signal transduction in olfactory neurons by attenuating activation of adenylyl cyclase III. Nature 409:1051.
[35] Noé, L., di Michele, M., Giets, E., Thys, C., Wittevrongel, C., de Vos, R., et al., 2010. Platelet Gs hypofunction and abnormal morphology resulting from a heterozygous RGS2 mutation. Journal of Thrombosis and Haemostasis 8(7): 1594—1603.
[36] Freson, K., Stolarz, K., Aerts, R., Brand, E., Brand-Herrmann, S.M., Kawecka-Jaszcz, K., et al., 2007. —391 C to G substitution in the regulator of G-protein signalling-2 promoter increases susceptibility to the metabolic syndrome in white European men: consistency between molecular and epidemiological studies. Journal of Hypertension 25(1):117—125.
[37] Yang, J., Kamide, K., Kokubo, Y., Takiuchi, S., Tanaka, C., Banno, M., et al., 2005. Genetic variations of regulator of G-protein signaling 2 in hypertensive patients and in the general population. Journal of Hypertension 23(8):1497—1505.
[38] Chikumi, H., Vazquez-Prado, J., Servitja, J.M., Miyazaki, H., Gutkind, J.S., 2002. Potent activation of RhoA by galpha q and gq-coupled receptors. Journal of Biological Chemistry 277(30):27130—27134.
[39] Lutz, S., Freichel-Blomquist, A., Yang, Y., Rumenapp, U., Jakobs, K.H., Schmidt, M., et al., 2005. The guanine nucleotide exchange factor p63RhoGEF, a specific link between Gq/11-coupled receptor signaling and RhoA. Journal of Biological Chemistry 280(12):11134—11139.
[40] Haas, B., Mayer, P., Jennissen, K., Scholz, D., Berriel Diaz, M., Bloch, W., et al., 2009. Protein kinase G controls brown fat cell differentiation and mitochondrial biogenesis. Science Signaling 2(99):ra78.
[41] McDonald, M.E., Li, C., Bian, H., Smith, B.D., Layne, M.D., Farmer, S.R., 2015. Myocardin-related transcription factor A regulates conversion of progenitors to beige adipocytes. Cell 160(1—2):105—118.
[42] Etienne-Manneville, S., Hall, A., 2002. Rho GTPases in cell biology. Nature 420(6916):629—635.
[43] Collins, S., 2014. A heart-adipose tissue connection in the regulation of energy metabolism. Nature Reviews Endocrinology 10(3):157—163.
[44] Nunn, C., Zhao, P., Zou, M.X., Summers, K., Guglielmo, C.G., Chidiac, P., 2011. Resistance to age-related, normal body weight gain in RGS2 deficient mice. Cellular Signalling 23(8):1375—1386.
[45] Granneman, J.G., 1995. Expression of adenylyl cyclase subtypes in brown adipose tissue: neural regulation of type III. Endocrinology 136(5):2007—2012.
[46] Rohlfs, E.M., Daniel, K.W., Premont, R.T., Kozak, L.P., Collins, S., 1995. Regulation of the uncoupling protein gene (Ucp) by beta 1, beta 2, and beta 3-adrenergic receptor subtypes in immortalized brown adipose cell lines. Journal of Biological Chemistry 270(18):10723—10732.
[47] Heximer, S.P., Blumer, K.J., 2007. RGS proteins: Swiss army knives in seven-transmembrane domain receptor signaling networks. Science's STKE 2007(370):pe2.
[48] Rosenwald, M., Wolfrum, C., 2014. The origin and definition of brite versus white and classical brown adipocytes. Adipocyte 3(1):4—9.
[49] Hudson, B.D., Shimpukade, B., Mackenzie, A.E., Butcher, A.J., Pediani, J.D., Christiansen, E., et al., 2013. The pharmacology of TUG-891, a potent and selective agonist of the free fatty acid receptor 4 (FFA4/GPR120), demonstrates both potential opportunity and possible challenges to therapeutic agonism. Molecular Pharmacology 84(5):710—725.

[50] Bodmann, E.L., Rinne, A., Brandt, D., Lutz, S., Wieland, T., Grosse, R., et al., 2014. Dynamics of Galphaq-protein-p63RhoGEF interaction and its regulation by RGS2. Biochemical Journal 458(1):131–140.

[51] Nobes, C.D., Hall, A., 1995. Rho, rac and cdc42 GTPases: regulators of actin structures, cell adhesion and motility. Biochemical Society Transactions 23(3): 456–459.

[52] Hall, A., 1998. Rho GTPases and the actin cytoskeleton. Science 279(5350): 509–514.

[53] Hartmann, S., Ridley, A.J., Lutz, S., 2015. The function of rho-associated kinases ROCK1 and ROCK2 in the pathogenesis of cardiovascular disease. Frontiers in Pharmacology 6(276).

[54] McBeath, R., Pirone, D.M., Nelson, C.M., Bhadriraju, K., Chen, C.S., 2004. Cell shape, cytoskeletal tension, and RhoA regulate stem cell lineage commitment. Developmental Cell 6(4):483–495.

[55] Hoffmann, L.S., Larson, C.J., Pfeifer, A., 2016. cGMP and Brown adipose tissue. Handbook of Experimental Pharmacology 233:283–299.

[56] Sun, X., Kaltenbronn, K.M., Steinberg, T.H., Blumer, K.J., 2005. RGS2 is a mediator of nitric oxide action on blood pressure and vasoconstrictor signaling. Molecular Pharmacology 67(3):631–639.

[57] Song, Y., Altarejos, J., Goodarzi, M.O., Inoue, H., Guo, X., Berdeaux, R., et al., 2010. CRTC3 links catecholamine signalling to energy balance. Nature 468: 933.

[58] Salim, S., Sinnarajah, S., Kehrl, J.H., Dessauer, C.W., 2003. Identification of RGS2 and type V adenylyl cyclase interaction sites. Journal of Biological Chemistry 278(18):15842–15849.

[59] Larminie, C., Murdock, P., Walhin, J.P., Duckworth, M., Blumer, K.J., Scheideler, M.A., et al., 2004. Selective expression of regulators of G-protein signaling (RGS) in the human central nervous system. Brain Research Molecular Brain Research 122(1):24–34.

[60] Kurrasch, D.M., Huang, J., Wilkie, T.M., Repa, J.J., 2004. Quantitative real-time polymerase chain reaction measurement of regulators of G-protein signaling mRNA levels in mouse tissues. In: Methods in enzymology. Academic Press. p. 3–15.

[61] Jennissen, K., Siegel, F., Liebig-Gonglach, M., Hermann, M.R., Kipschull, S., van Dooren, S., et al., 2012. A VASP-Rac-soluble guanylyl cyclase pathway controls cGMP production in adipocytes. Science Signaling 5(239):ra62.

